ACS OMEGA

http://pubs.acs.org/journal/acsodf

Article

Lightweight Epoxy/Cotton Fiber-Based Nanocomposites with Carbon and Fe_3O_4 for Electromagnetic Interference Shielding

Jianwei Xu, Ruiyue Chen, Zhigeng Yun, Zhongyi Bai, Kun Li, Shaozhe Shi, Junji Hou,* Xiaoqin Guo, Xiaoli Zhang,* and Jingbo Chen*

Cite This: *ACS Omega* 2022, 7, 15215−15222

Read Online

ACCESS | Metrics & More | Article Recommendations | Supporting Information

ABSTRACT: Cotton fiber (CF)-based electroconductive papers were prepared by facile aqueous dispersion and drying processes combined with carbon nanotubes (CNTs) or graphene nanosheets (GNPs). To enhance the electromagnetic interference (EMI) shielding performance of the manufactured nanocomposites, the electroconductive papers were soaked with epoxy resin, which cooperated with the inner sprayed Fe_3O_4 nanoparticles. The EMI shielding effectiveness of Epoxy/CF-30-Fe_3O_4-30GNPs reached 33.1 dB, of which over 85.0% is attributed to absorption, which is mainly believed to be caused by the combination of GNPs and Fe_3O_4 nanoparticles due to their special structures and synergetic effects. Moreover, the infiltration of epoxy between the randomly distributed loose CFs and the multiple reflections inside the interconnected networks could also help to improve the EMI shielding performance of GNP-added samples. The prepared lightweight and stiff Epoxy/CF-30-Fe_3O_4-30GNP composites have promising applications in civil or military fields.

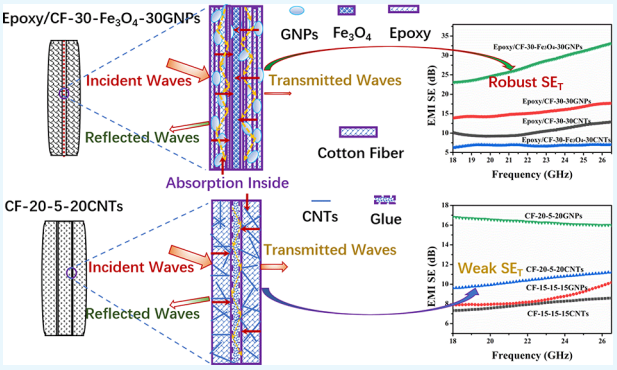

1. INTRODUCTION

Being one of the rapidly increasing pollutions induced by the inventions of advanced electronic information technology, electromagnetic (EM) pollution is becoming a potential serious hazard to human beings and adjacent precision electronic equipment.[1−5] To maximally eliminate or reduce the damage of such EM pollutions, novel electromagnetic interference (EMI) shielding materials, such as electrically conductive polymer composites (CPCs),[6−12] intrinsically conducting polymers (ICP), MXenes,[13−17] and textile or paper-shaped materials, have been successively developed in the past decade.[8,18,19] Compared with traditional metal EMI shielding materials, the above EMI shielding protection categories have the advantages of lightweight, corrosion resistance, and flexible processability.[13,20−23] Among them, carbon-based electroconductive papers arise promisingly due to their superior features, such as low cost, balanced mechanical properties, easy formability, and excellent service condition adaptability.[15,21,24,25] Using renewable biomass as an applicable component in CPCs is one of the most promising alternatives, with respect to the green ecological development tendency and the current requirements for the fabrication of multifunctional EMI shields.[7,13,15,21]

Cellulose fibers are renewable natural materials with abundant reserves, which are frequently involved in paper and pulp making industries.[26] The superior biodegradability, hydrophilicity, and low toxicity of the papers made from cellulose fibers make them one of the prospective substrates for EMI shielding composites.[7,8,15,27,28] In general, the key factor to endow cellular paper with conductivity is the addition of conductive additives, such as conductive nanoparticles or fibers, among which carbon-based materials, like carbon black (CB), carbon nanotubes (CNTs), graphene nanosheets (GNPs), and carbon fibers (CFs), are usually used.[8,29−34] CNTs are one-dimensional carbon materials with a high aspect ratio, which have been chosen as an effective nanoscale functional filler to produce polymer- or natural cellulose fiber-based conductive nanocomposites[35] due to their exceptional electric conductivity, thermal stability, and mechanical properties.[36−39] GNPs are two-dimensional carbon nanosheets that are also frequently used in the fabrication of conductive nanocomposites because of their super high specific surface area, exceptional carrier mobility, and excellent ballistic electron transport property.[19,20,39−41] Typically, carbon-filled cellulose composite papers derived from a facile papermaking

Received: March 10, 2022
Accepted: April 11, 2022
Published: April 20, 2022

technology are known to be eco-friendly materials, compared with the ionic or toxic polar solvents involved in fabricating processes.[27,30] Lee et al.[27] prepared a series of multiwalled carbon nanotube (MWCNT)-coated cellulose papers by using the dip-coating process. The influences of dip-coating cycles (from 1 to 30) on the EMI shielding performance and electric conductivity were investigated, showing that both EMI shielding effectiveness (SE) and electric conductivity of MWCNT/cellulose papers increased with increasing dip-coating cycles. The highest EMI shielding effectiveness of 20.3 dB and an electric conductivity of 1.11 S/cm were achieved with a dip-coating cycle of 30. Jia et al.[42] reported a high EMI shielding effectiveness of 46.0−82.0 dB for epoxy coating-reinforced carbonized waste corrugated boards. Lu et al.[43] produced a nonwoven fabric CEF-NF (nonwoven fabric) with 40 wt % CF (carbon fiber) and an area density of 50 g/m^2, through a two-step wet-papermaking/thermal-bonding process. A total EMI shielding value of 30.29 dB was achieved for the composite in the frequency range of 30−1500 MHz.

According to previous reports, filter papers were applied as templates for EMI shielding purposes, but they usually have a large-scale processing limitation.[6,8] The use of cellulose fibers in composites is a promising direction for the production of lightweight EMI shielding materials.[8,21,27] In this study, a facile method, similar to the traditional wet-papermaking process, was adopted to fabricate the lightweight cellulose fiber-based electroconductive papers, in which CNTs or GNPs were used as conductive fillers. To avoid the negative transmitted effects of the conductive papers, epoxy was further used to fill the small pores around the anisotropically distributed cellulose fibers. Furthermore, ferromagnetic nanoparticles were sprayed onto the surface of one epoxy-dipped conductive paper, before clinging with another conductive paper. The characteristics of the obtained EMI shielding composites were also investigated. The results show that comparatively high EMI shielding performances of such nanocomposites can be achieved, through this cheap, easy, and green processing strategy, which cooperated with a synergism shielding mechanism.

2. RESULTS AND DISCUSSION

2.1. Morphologies of the Cellulose Fiber-Based Conductive Papers. Based on the facile preparation process of the fiber-based conductive composites, different cotton fiber-loaded electrically conductive papers were produced, and the morphologies of these conductive papers are presented in Figure 1. Figure 1a,b shows the surfaces of CF-20CNT conductive papers. Compared to the non-CNT-loaded original fibers (Figure S1), looser, rougher, and more randomly distributed cotton fibers were captured, as indicated by the arrows.

Due to the existence of abundant hydroxyl groups in cotton fibers, CNTs could be easily attracted to the surfaces of these micro-sized cellulose fibers. The relatively uniform brightness of the CNT-coated papers in Figure 1 indicates the good conductive properties of the manufactured samples, which assisted with the construction of the electrically conductive circuits or channels, through the fine distribution of the CNTs. Figure 1c,d shows the morphologies of CF-20GNP papers; because of the two-dimensional structures of the GNPs, comparatively smooth cotton fiber surfaces and irregular fiber distribution, similar to the case of CNT-loaded conductive papers, can be identified, as illustrated in the ellipse.

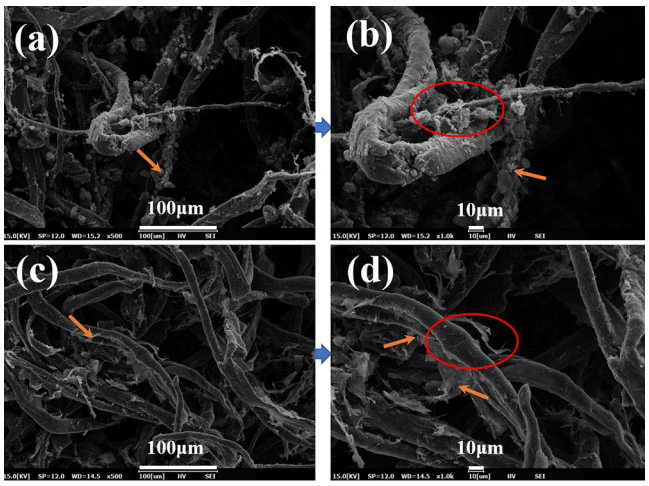

Figure 1. SEM pictures of (a) CF-20CNTs and (c) CF-20GNPs; (b) and (d) are the enlarged pictures of (a) and (b), correspondingly.

2.2. Performance of the Cellulose Fiber-Based Conductive Papers. The electric conductivities of the CF-CNT and CF-GNP papers are presented in Figure 2. It is very

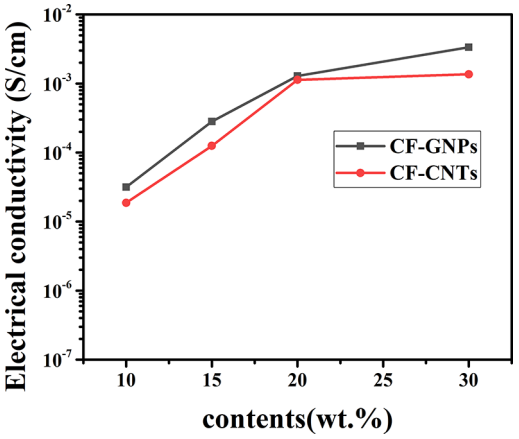

Figure 2. Electric conductivities of CF-CNTs and CF-GNPs, with different carbon contents.

clear that the electric conductivity of CF-based papers increased gradually with increasing contents of CNTs or GNPs. For the one-layered conductive papers with a thickness of around 1.0 mm, the tested SE values are shown in Figure 3, which are relatively low (below 10.0 dB) and not ideal for commercial EMI shielding applications. The EMI shielding performance of GNP-loaded papers is higher than that of the CNT-added samples at the same loading level, which is mainly attributed to the better conductive circuits constructed by the two-dimensional sheet structures of the GNPs, compared to that of CNTs. It should be noted that absorptions are the dominating shielding mechanisms, as shown in Figure S2.

In particular, the comparisons of EMI shielding performance between one- and three-layered composites are illustrated in Figure S3, showing that the SE values of the latter (thicker) ones increased dramatically faster than the one-layered composites, when tested in the same frequency zone. To further compare the influence of the sample thickness and carbon contents on the EMI shielding effectiveness, the EMI SE values of three-layered composites with different cotton

https://doi.org/10.1021/acsomega.2c01293
ACS Omega 2022, 7, 15215−15222

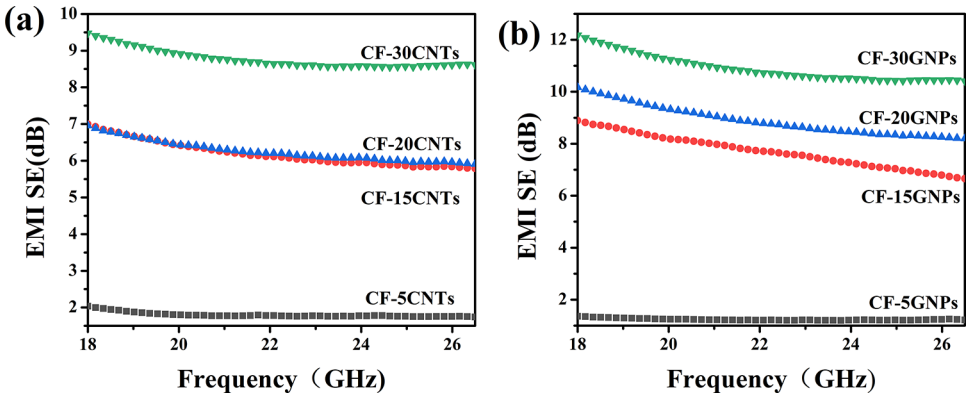

Figure 3. EMI SE (shielding effectiveness) of one-layered composites (a) CF-CNTs and (b) CF-GNPs (the average thickness of the compressed samples is 1.0 ± 0.1 mm).

contents are shown in Figure S4. The average thickness of the obtained three-layered composites is in the range of 3.6−4.0 mm, laminated by glue. As shown, the highest SE_T value was found for the sample CF-20-5-20GNPs, which was 16.8 dB at a frequency of 18 GHz (Figure S4a); it is obviously higher than that of the one-layered composite in Figure 3. In the cases of CNT-coated samples, the EMI efficiencies are all below 11.0 dB at 18 GHz, which is much lower than that of the commercially accepted limitation of 20.0 dB. Figure S4b presents the SE_T, SE_A, and SE_R values of the three-layered samples of CF-15-15-15CNTs (for convenient comparison and control of the sample thickness, we used three CF-15CNT composite samples herein) and CF-20-5-20CNTs, showing that the absorptions are still the predominant mechanisms in these CF-based EMI shielding materials. For example, at a frequency of 26.0 GHz, the SE_T, SE_A, and SE_R values for the sample CF-20-5-20CNTs are 11.2, 9.7, and 1.5 dB, respectively, which indicate the absolute dominance of absorption (86.6%). Compared to CF-15-15-15CNTs, with a CNT distribution gradient in CF-20-5-20CNTs, the conductive network could be rearranged, and multiple reflections in the adjacent layers might be induced; thus, the EMI shielding performances are improved compared with those of CF-15-15-15CNTs. As the highest SE value among these one- and three-layered conductive papers is still lower than that of the commercially accepted requirement, the EMI shielding performance of the electrically conductive papers obtained in this section (similar to the literature) is not suitable for practical applications, which should be modified to meet the commercial demand.[27,40]

2.3. Performance and EMI Shielding Mechanism of Epoxy-Soaked Composites. To fabricate CF-based EMI shielding composites with high efficiency, Fe_3O_4 nanoparticles were generally used as a magnetic loss effect resource, which might interact with the coupled electric and magnetic (EM) radiation fields.[43] Figure 4 shows the X-ray graphs of CF-CNTs/GNPs, as well as the Fe_3O_4-sprayed CF-CNT samples. The existence of the peaks at 2θ = 30.12, 35.46, 43.08, 53.73, 57.26, and 62.73° for CF-20CNTs-5Fe_3O_4 indicated the successful introduction of Fe_3O_4, which correspond to the (220), (311), (400), (422), (511), and (440) planes of the Fe_3O_4 crystal, respectively, as presented in our previous study and the literature.[11,44] The diffraction peaks in the (002) planes are attributed to the presence of graphite.[10,11,45] Meanwhile, peaks in the (020) plane, at 2θ = 22.6°, are typical signals of cellulose fibers (Figure S5).[46]

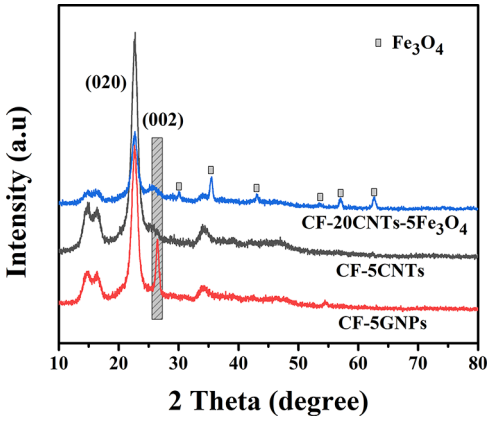

Figure 4. XRD graphs of CF-20CNTs-5Fe_3O_4, CF-5CNTs, and CF-5GNPs.

As illustrated previously, conductive cellulose papers with a high CNT or GNP content of 30 wt % could not achieve the ideal EMI shielding performance, partially due to their loose structure. To improve the EMI shielding effectiveness of these composites, epoxy resin was used to fill the crevices or cells between the CF fibers, cooperating with a 5 wt % Fe_3O_4 layer sprayed in the interface of two CF-CNT or CF-GNP papers. After curing and pressing, a special sandwich structure of the CF-based composites was produced, and a relatively stiff feature of the Epoxy/CF-Fe_3O_4-CNTs (GNPs) was obtained.[40] Figure 5 shows the SEM pictures of the fractured Epoxy/CF-30-Fe_3O_4-30GNP composite surfaces. The holes and concaves presented in Figure 1 were filled by epoxy, which is critical for the improvement of the EMI shielding performance because the epoxy could prevent the direct penetration of the incident waves through the holes and concaves originally. Furthermore, cooperating with the reconstruction of the conductive circuits, the EMI shielding performance of the cotton fiber-based nanocomposites could be clearly enhanced, as further illustrated. The fractured cross sections of the composites are rather coarse, and the fibers were tightly anchored in the epoxy basement, which could absorb energy during the fracturing process, so rough fiber section shapes could be obviously identified, pointed by the arrows in Figure 5. Herein, the epoxy not only provided a barrier to prevent the penetration of the incident electromagnetic waves but also offered a strong casting base to

https://doi.org/10.1021/acsomega.2c01293
ACS Omega 2022, 7, 15215−15222

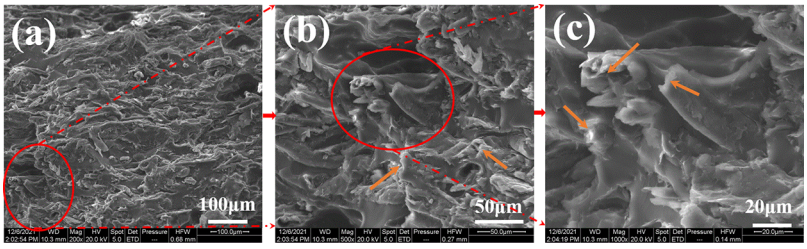

Figure 5. SEM pictures of Epoxy/CF-30-Fe_3O_4-30GNPs with different magnifications: (a) 200×, (b) 500×, and (c) 1000×.

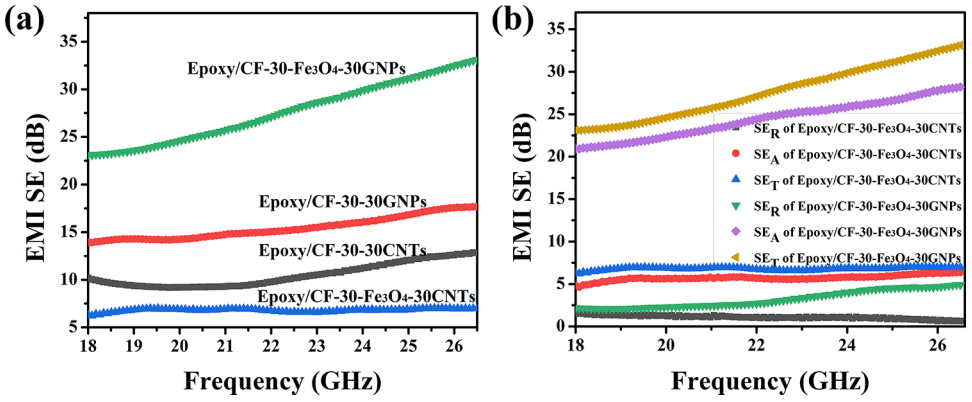

Figure 6. EMI SE performance of sandwich Epoxy/CF-30-30CNT and Epoxy/CF-30-30GNP composites (the average thickness is 2.58 mm) with or without Fe_3O_4 nanoparticles: (a) EMI SE and (b) SE_T, SE_A, and SE_R (the average thickness of the Fe_3O_4-loaded samples is 2.68 mm).

produce stiff nanocomposites, which can withstand the harsh service circumstances.

The EMI SE efficiency graphs of the manufactured samples are presented in Figure 6. The robust EMI shielding performance of Epoxy/CF-30-Fe_3O_4-30GNPs can be found from Figure 6a,b. Interestingly, the SE_T of the Epoxy/CF-30-Fe_3O_4-30CNTs is much lower than that of Epoxy/CF-30-Fe_3O_4-30GNPs in the whole test frequency range. We speculate that the introduction of epoxy and Fe_3O_4 nanoparticles blocked some electrically conductive circuits, in the cases of CNT-added samples, mainly because of their one-dimensional structure, which is rather different from that of the GNPs. For the GNP-coated case of Epoxy/CF-30-Fe_3O_4-30GNPs with a thickness of 2.68 mm, the two-dimensional structures and mass surfaces of GNPs could help to broaden the transition scope of the electrons, both in in-plane and cross-sectional directions, as illustrated in Figure 7. In other words, the mass surfaces could positively provide chances for multiple internal reflections and scatterings, both around the cellulose fibers and in the interlayered surfaces of the GNPs, between the directions of alignment as well as perpendicular to them, through the "tunneling" effects.[43] Furthermore, the distribution of Fe_3O_4 nanoparticles could be magnified to affect the magnetic loss.[11,45] Thus, the average SE_T value of the GNP-added samples (33.1 dB at a frequency of 26.5 GHz) is much higher than that of the CNT-coated counterparts in the same frequency range, so we can draw a conclusion that the synergetic effect of the dielectric loss, magnetic loss, and multiple reflections on the interlayered surfaces causes this higher SE value of 33.1 dB. The results in Figure S6 can also positively prove our conjectures; the SE_T values of Epoxy/CF-10CNTs and Epoxy/CF-10GNPs are rather lower than that of Epoxy/CF-30GNPs. Moreover, the highest SE_T of Epoxy/CF-30-30GNPs in Figure 6a, at a frequency of 26.5 GHz, is 15.5 dB, which is much lower than the shielding efficiency of its

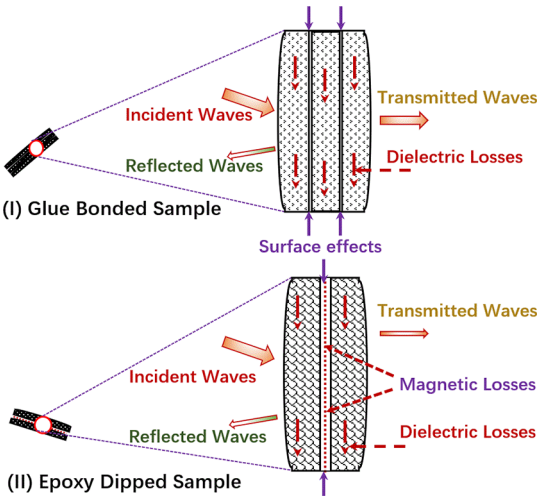

Figure 7. Schematic SEM interference mechanism illustration of the two composites.

Fe_3O_4-filled counterpart. Clearly, Fe_3O_4 nanoparticles play a crucial role in achieving the high EMI shielding performance in the case of Epoxy/CF-30-Fe_3O_4-30GNPs.

Figure 6b exhibits the components of EMI effectiveness of epoxy-soaked composites; as expected, SE_A is the dominating shielding mechanism, which is in favor of avoiding the potential secondary pollution, mainly induced by the reflection waves.[11] These results can be ascribed to the multifunctional effects of the sandwich structures of the Epoxy/CF-30-Fe_3O_4-30GNPs, which could trigger multiple reflections between different layers and bulky surfaces of randomly distributed cellulose fibers and GNPs. This Epoxy/CF-30-Fe_3O_4-30GNP composite has advantages of lightweight, stiffness, and low

https://doi.org/10.1021/acsomega.2c01293
ACS Omega 2022, 7, 15215−15222

cost, which can make it a promising prospective material in the related EM radiation protection areas.

3. CONCLUSIONS

In summary, lightweight cellulose cotton fiber-based EMI shielding nanocomposites were prepared by combining them with carbons and Fe_3O_4 nanoparticles, clung with glue or epoxy. The highest EMI performance of 33.1 dB at a frequency of 26.5 GHz was achieved for the sandwich-structured Epoxy/CF-30-Fe_3O_4-30GNP nanocomposites. The excellent EMI shielding efficiency was derived from the synergetic effects of the dielectric loss, magnetic loss, multiple reflections, scattering, and impedance matching. The filling of epoxy in the micro-sized pores between cotton fibers could obviously improve the EMI shielding performance of the GNP-coated composites. Compared to the CNT- and Fe_3O_4 nanoparticle-filled samples, much higher EMI values were measured for the GNP-coated samples, which are attributed to the special two-dimensional structure and the mass surface areas of the GNPs. Thus, the obtained lightweight nanocomposites have promising applications in the areas of novel electronics, aerospace, and military stealth equipment.

4. EXPERIMENTAL SECTION

4.1. Materials. Cotton fibers with an average length of 2.0−3.0 mm and a width of 15−20 μm (Figure S1) were supplied by the China National Pulp and Paper Research Institute, originally planted in the Hebei province of China. The received pulp cotton fibers were manufactured through an alkali treatment and three-stage bleaching, after removing lignin and colloids, retaining most of the cellulose and semicellulose.[47] Carbon nanotubes (CNTs), with the trade number TNM2 (manufactured by Chengdu Organic Chemicals Co., Ltd., Chinese Academy of Sciences, China) were used as the electrically conductive filler, with a purity of >95%. The outer diameter of the CNTs was in the range of 8−15 nm, and the length was about 50 μm. Graphene nanosheets (GNPs) were purchased from Aladdin Co., Ltd., Shanghai, with a purity of >99.5%. Fe_3O_4 nanoparticles with an average diameter of 20 nm were bought from Maikelin Biochemistry Company, with a purity of >99.5%. Epoxy and the curing agent were homemade products, provided by the Product Engineering Department of Zhengzhou Yutong Bus Co., Ltd., and PVAL glue was produced by Deli Group Co., Ltd.

4.2. Preparation of the EMI Shielding Composites. According to the multifunctional mechanisms of high EMI shielding composites, electric conductivity is a predominant factor that can be achieved through the addition of CNTs or GNPs, as mentioned above. Also, the magnetic property is another influencing element that can affect the EMI efficiency. Fe_3O_4 nanoparticles are recognized as a group of cheap and effective additives that are frequently used in the fabrication of magnetic materials to improve the magnetic losses.[10,11,45,48] Moreover, the surface feature is another key factor, which should be carefully considered in the fabrication of EMI shielding composites.[14,49] On the basis of mechanism-oriented design conception, two fabrication methods had been applied in this work. On the one side, the CNT- or GNP-added conductive papers were simply bonded by glue (way I in Figure 7). On the other side, epoxy was introduced to fill the textile pores, and Fe_3O_4 was sprayed to enhance the EMI shielding efficiency (way II in Figure 7). Finally, the EMI shielding properties of the prepared samples were tested and compared subsequently.

The detailed fabrication processes of the cotton fiber-based EMI shielding nanocomposites are schematically illustrated in Figure 8. To prepare the electrically conductive cellulose papers, cotton fibers (1.5 g weighted) were first added into 100 mL of deionized water to obtain the CF suspensions, in which different contents of CNTs/GNPs (for example, in a 10 wt % CNT-filled cotton fiber paper, CNTs and fibers were 0.15 and 1.35 g weighted, respectively) were added under ultrasonic stirring. After that, the obtained CF/CNT or CF/GNP suspensions were heated to 100 °C to evaporate water and get porous cakes from them. After several heating operations in a vacuum oven at 80 °C for 4 h each before a constant measurement, the electrically conductive CF-based papers were pressed to a circle shape, with an average diameter of 60 mm and a thickness of about 1.0 mm, under a pressure of 10 MPa at a room temperature of 25 °C and a humidity of 30%. To prepare multilayer CF-based conductive papers with different internal structures, the glue clinging and epoxy dipping methods were applied, as shown in Figure 8-② and Figure 8-③. For curing of the epoxy-dipped samples (the weight ratio of the epoxy and the curing agent was 5:1), the oven was preheated to 60 °C, and the samples were loaded and held for 30 min; after that, the oven temperature was elevated in sequence to 120 and 130 °C and held for 30 min at each temperature, intermittently. Finally, the obtained multilayer CF-based papers were pressed tightly using a laboratory press under a pressure of 10 MPa, at room temperature.

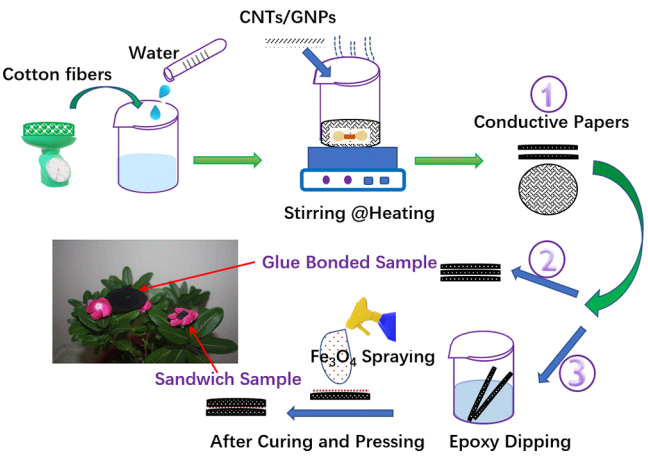

Figure 8. Schematic illustration of the sample preparation.

The samples were demonstrated by indicating the weight content of individual carbon components. For example, a sample code of CF-15-15-15CNTs refers to a three-layered CF composite coated with CNTs in each layer and the CNT contents are 15 wt % individually, in which the three of them were clung together by glue. The Epoxy/CF-30-Fe_3O_4-30GNP sample is a two-layered nanocomposite with a 30 wt % GNP content coated in each layer and 5 wt % Fe_3O_4 sprayed between them. These two layers were soaked with epoxy resin and compressed together using the same laboratory press finally.

4.3. Characterization. The morphologies of the prepared CNT- and GNP-added conductive CF-based papers as well as the epoxy-soaked nanocomposites were scanned by a field-emission scanning electron microscope (SEM, EM-30Plus,

https://doi.org/10.1021/acsomega.2c01293
ACS Omega 2022, 7, 15215−15222

COXEM Company, Korea). X-ray diffraction (XRD) tests were carried out by using an X-ray diffractometer (Rigaku Ultima IV, Japan) with Cu Kα (λ = 1.5418 Å) radiation with a voltage of 40 kV and a current of 40 mA, to examine the phase compositions of the nanocomposites, in the scanning range of 10−80°.

The electric conductivities of the cellulose conductive papers were measured by a Tektronix DMM4050. The EMI shielding performance was investigated using a vector network analyzer (VNA, Agilent N5234A) at room temperature, combined with two face-to-face waveguide-to-coaxial adaptors, in the range of 18−26.5 GHz (Ku band).[10] The VNAS scattering parameter was calibrated before the measurements. The samples that must be measured were cut into a rectangle shape with a size of 10.6 mm (length) × 4.3 mm (width) to match the waveguide holders. The incident electromagnetic wave power was 0 dBm, corresponding to 1 mW. The EMI parameters SE total, SE reflection, and SE absorption (SE_T, SE_R, and SE_A, respectively) were calculated from S_{11} and S_{21}.[13,27]

$$R = |S_{11}|^2 \quad (1)$$

$$T = |S_{21}|^2 \quad (2)$$

$$A = 1 - R - T \quad (3)$$

$$SE_R = -10 \log(1 - R) \quad (4)$$

$$SE_A = -10 \log\left[\frac{T}{1 - R}\right] \quad (5)$$

$$SE_T = SE_R + SE_A \quad (6)$$

ASSOCIATED CONTENT

Supporting Information

The Supporting Information is available free of charge at https://pubs.acs.org/doi/10.1021/acsomega.2c01293.

Fiber morphology (SEM picture), EMI shielding, and various EM parameters of the composites, as well as 1D WAXD graphs of cotton fibers (PDF)

AUTHOR INFORMATION

Corresponding Authors

Junji Hou − *School of Materials Science and Engineering, Zhengzhou University, Zhengzhou 450001, China*; Email: junjihou@zzu.edu.cn

Xiaoli Zhang − *School of Materials Science and Engineering, Zhengzhou University, Zhengzhou 450001, China*; orcid.org/0000-0003-3301-644X; Email: zhangxl@zzu.edu.cn

Jingbo Chen − *School of Materials Science and Engineering, Zhengzhou University, Zhengzhou 450001, China*; Email: chenjb@zzu.edu.cn

Authors

Jianwei Xu − *School of Materials Science and Engineering, Zhengzhou University, Zhengzhou 450001, China*

Ruiyue Chen − *School of Materials Science and Engineering, Zhengzhou University, Zhengzhou 450001, China*

Zhigeng Yun − *School of Materials Science and Engineering, Zhengzhou University, Zhengzhou 450001, China*

Zhongyi Bai − *School of Materials Science and Engineering, Henan Key Laboratory of Aeronautical Materials and Application Technology, Zhengzhou University of Aeronautics, Zhengzhou 450046, China*

Kun Li − *School of Materials Science and Engineering, Zhengzhou University, Zhengzhou 450001, China*

Shaozhe Shi − *School of Materials Science and Engineering, Zhengzhou University, Zhengzhou 450001, China; College of Polymer Science and Engineering, State Key Laboratory of Polymer Materials Engineering, Sichuan University, Chengdu 610065, China*

Xiaoqin Guo − *School of Materials Science and Engineering, Henan Key Laboratory of Aeronautical Materials and Application Technology, Zhengzhou University of Aeronautics, Zhengzhou 450046, China*

Complete contact information is available at: https://pubs.acs.org/10.1021/acsomega.2c01293

Notes

The authors declare no competing financial interest.

ACKNOWLEDGMENTS

The authors sincerely appreciate the National Natural Science Foundation of China (11872338 and U1804144), the Henan Province Natural Science Project of China (21A430039 and 212102210207), and the Fundamental Research Funds for the Central Universities (Grant No. 20826041E4280) for their financial support.

REFERENCES

(1) Sheng, A.; Ren, W.; Yang, Y.; Yan, D.-X.; Duan, H.; Zhao, G.; Liu, Y.; Li, Z.-M. Multilayer WPU conductive composites with controllable electro-magnetic gradient for absorption-dominated electromagnetic interference shielding. *Composites, Part A* **2020**, *129*, No. 105692.

(2) Xu, C.; Wu, F.; Xie, A.; Duan, L.; Yang, Z.; Xia, Y.; Sun, M.; Xiong, Z. Hollow polypyrrole nanofiber-based self-assembled aerogel: large-scale fabrication and outstanding performance in electromagnetic pollution management. *Ind. Eng. Chem. Res.* **2020**, *59*, 7604−7610.

(3) Tang, W.; Lu, L.; Xing, D.; Fang, H.; Liu, Q.; Teh, K. S. A carbon-fabric/polycarbonate sandwiched film with high tensile and EMI shielding comprehensive properties: An experimental study. *Composites, Part B* **2018**, *152*, 8−16.

(4) Chen, W.; Liu, L. X.; Zhang, H. B.; Yu, Z. Z. Kirigami-inspired highly stretchable, conductive, and hierarchical $Ti_3C_2T_x$ MXene films for efficient electromagnetic interference shielding and pressure sensing. *ACS Nano* **2021**, *15*, 7668−7681.

(5) Menon, A. V.; Madras, G.; Bose, S. Ultrafast self-healable interfaces in polyurethane nanocomposites designed using diels-alder "Click" as an efficient microwave absorber. *ACS Omega* **2018**, *3*, 1137−1146.

(6) Zhang, J.; Qi, Y.; Zhang, Y.; Duan, J.; Liu, B.; Liu, B.; Sun, Z.; Xu, Y.; Hu, W.; Zhang, N. Lignin based flexible electromagnetic shielding PU synergized with graphite. *Fibers Polym.* **2021**, *22*, 1−8.

(7) Luo, H.; Xie, J.; Xiong, L.; Zhu, Y.; Yang, Z.; Wan, Y. Fabrication of flexible, ultra-strong, and highly conductive bacterial cellulose-based paper by engineering dispersion of graphene nanosheets. *Composites, Part B* **2019**, *162*, 484−490.

(8) Mondal, S.; Ganguly, S.; Das, P.; Bhawal, P.; Das, T. K.; Nayak, L.; Khastgir, D.; Das, N. C. High-performance carbon nanofiber coated cellulose filter paper for electromagnetic interference shielding. *Cellulose* **2017**, *24*, 5117−5131.

(9) Ameli, A.; Kazemi, Y.; Wang, S.; Park, C. B.; Pötschke, P. Process-microstructure-electrical conductivity relationships in injection-molded polypropylene/carbon nanotube nanocomposite foams. *Composites, Part A* **2017**, *96*, 28−36.

(10) Zhao, Y.; Hou, J.; Bai, Z.; Yang, Y.; Guo, X.; Cheng, H.; Zhao, Z.; Zhang, X.; Chen, J.; Shen, C. Facile preparation of lightweight PE/PVDF/Fe_3O_4/CNTs nanocomposite foams with high conductivity for efficient electromagnetic interference shielding. *Composites, Part A* **2020**, *139*, No. 106095.
(11) Cheng, H.; Wei, S.; Ji, Y.; Zhai, J.; Zhang, X.; Chen, J.; Shen, C. Synergetic effect of Fe_3O_4 nanoparticles and carbon on flexible poly (vinylidence fluoride) based films with higher heat dissipation to improve electromagnetic shielding. *Composites, Part A* **2019**, *121*, 139−148.
(12) Anju; Yadav, R. S.; Potschke, P.; Pionteck, J.; Krause, B.; Kuritka, I.; Vilcakova, J.; Skoda, D.; Urbanek, P.; Machovsky, M.; Masar, M.; Urbanek, M.; Jurca, M.; Kalina, L.; Havlica, J. High-performance, lightweight, and flexible thermoplastic polyurethane nanocomposites with Zn(2+)-substituted $CoFe_2O_4$ nanoparticles and reduced graphene oxide as shielding materials against electromagnetic pollution. *ACS Omega* **2021**, *6*, 28098−28118.
(13) Jia, X.; Shen, B.; Zhang, L.; Zheng, W. Waterproof MXene-decorated wood-pulp fabrics for high-efficiency electromagnetic interference shielding and Joule heating. *Composites, Part B* **2020**, *198*, No. 108250.
(14) Xie, F.; Jia, F.; Zhuo, L.; Lu, Z.; Si, L.; Huang, J.; Zhang, M.; Ma, Q. Ultrathin MXene/aramid nanofiber composite paper with excellent mechanical properties for efficient electromagnetic interference shielding. *Nanoscale* **2019**, *11*, 23382−23391.
(15) Hu, D.; Huang, X.; Li, S.; Jiang, P. Flexible and durable cellulose/MXene nanocomposite paper for efficient electromagnetic interference shielding. *Compos. Sci. Technol.* **2020**, *188*, No. 107995.
(16) Ma, C.; Liu, T.; Xin, W.; Xi, G.-Q.; Ma, M.-G. Breathable and wearable MXene-decorated air-laid paper with superior folding endurance and electromagnetic interference-shielding performances. *Front. Mater.* **2019**, *6*, 308.
(17) Xu, M.-K.; Liu, J.; Zhang, H.-B.; Zhang, Y.; Wu, X.; Deng, Z.; Yu, Z.-Z. Electrically conductive $Ti_3C_2T_x$ MXene/polypropylene nanocomposites with an ultralow percolation threshold for efficient electromagnetic interference shielding. *Ind. Eng. Chem. Res.* **2021**, *60*, 4342−4350.
(18) Duan, H.; Zhu, H.; Yang, J.; Gao, J.; Yang, Y.; Xu, L.; Zhao, G.; Liu, Y. Effect of carbon nanofiller dimension on synergistic EMI shielding network of epoxy/metal conductive foams. *Composites, Part A* **2019**, *118*, 41−48.
(19) Hamidinejad, M.; Zhao, B.; Zandieh, A.; Moghimian, N.; Filleter, T.; Park, C. B. Enhanced electrical and electromagnetic interference shielding properties of polymer-graphene nanoplatelet composites fabricated via supercritical-fluid treatment and physical foaming. *ACS Appl. Mater. Interfaces* **2018**, *10*, 30752−30761.
(20) Wang, W. Y.; Ma, X.; Shao, Y. W.; Qi, X. D.; Yang, J. H.; Wang, Y. Flexible, multifunctional, and thermally conductive nylon/graphene nanoplatelet composite papers with excellent EMI shielding performance, improved hydrophobicity and flame resistance. *J. Mater. Chem. A* **2021**, *9*, 5033−5044.
(21) Li, E.; Pan, Y.; Wang, C.; Liu, C.; Shen, C.; Pan, C.; Liu, X. Multifunctional and superhydrophobic cellulose composite paper for electromagnetic shielding, hydraulic triboelectric nanogenerator and Joule heating applications. *Chem. Eng. J.* **2021**, *420*, No. 129864.
(22) Chen, J.; Liao, X.; Xiao, W.; Yang, J.; Jiang, Q.; Li, G. Facile and green method to structure ultralow-threshold and lightweight polystyrene/MWCNT composites with segregated conductive networks for efficient electromagnetic interference shielding. *ACS Sustainable Chem. Eng.* **2019**, *7*, 9904−9915.
(23) Tran, M.-P.; Thomassin, J.-M.; Alexandre, M.; Jerome, C.; Huynen, I.; Detrembleur, C. Nanocomposite foams of polypropylene and carbon nanotubes: preparation, characterization, and evaluation of their performance as EMI absorbers. *Macromol. Chem. Phys.* **2015**, *216*, 1302−1312.
(24) Kargarzadeh, H.; Huang, J.; Lin, N.; Ahmad, I.; Mariano, M.; Dufresne, A.; Thomas, S.; Gałęski, A. Recent developments in nanocellulose-based biodegradable polymers, thermoplastic polymers, and porous nanocomposites. *Prog. Polym. Sci.* **2018**, *87*, 197−227.
(25) Ghosh, K.; Srivastava, S. K. Enhanced supercapacitor performance and electromagnetic interference shielding effectiveness of CuS quantum dots grown on reduced graphene oxide sheets. *ACS Omega* **2021**, *6*, 4582−4596.
(26) Cheng, C.; Guo, R.; Tan, L.; Lan, J.; Jiang, S.; Du, Z.; Zhao, L. A bio-based multi-functional composite film based on graphene and lotus fiber. *Cellulose* **2019**, *26*, 1811−1823.
(27) Lee, T.-W.; Lee, S.-E.; Jeong, Y. G. Carbon nanotube/cellulose papers with high performance in electric heating and electromagnetic interference shielding. *Compos. Sci. Technol.* **2016**, *131*, 77−87.
(28) Fei, Y.; Liang, M.; Chen, Y.; Zou, H. Sandwich-like magnetic graphene papers prepared with MOF-derived Fe_3O_4−C for absorption-dominated electromagnetic interference shielding. *Ind. Eng. Chem. Res.* **2019**, *59*, 154−165.
(29) Ju, J.; Kuang, T.; Ke, X.; Zeng, M.; Chen, Z.; Zhang, S.; Peng, X. Lightweight multifunctional polypropylene/carbon nanotubes/carbon black nanocomposite foams with segregated structure, ultralow percolation threshold and enhanced electromagnetic interference shielding performance. *Compos. Sci. Technol.* **2020**, *193*, No. 108116.
(30) Ma, X.; Shen, B.; Zhang, L.; Liu, Y.; Zhai, W.; Zheng, W. Porous superhydrophobic polymer/carbon composites for lightweight and self-cleaning EMI shielding application. *Compos. Sci. Technol.* **2018**, *158*, 86−93.
(31) Sun, T.; Luo, W.; Luo, Y.; Wang, Y.; Zhou, S.; Liang, M.; Chen, Y.; Zou, H. Self-reinforced polypropylene/graphene composite with segregated structures to achieve balanced electrical and mechanical properties. *Ind. Eng. Chem. Res.* **2020**, *59*, 11206−11218.
(32) Sedighi, A.; Taheri, R. A.; Montazer, M. High-performance electromagnetic interference shielding electrodes/substrates for wearable electronics. *Ind. Eng. Chem. Res.* **2020**, *59*, 12774−12783.
(33) Sultana, S. M. N.; Pawar, S. P.; Sundararaj, U. Effect of processing techniques on EMI SE of immiscible PS/PMMA blends containing MWCNT: enhanced intertube and interphase scattering. *Ind. Eng. Chem. Res.* **2019**, *58*, 11576−11584.
(34) Wang, G.; Yu, Q.; Hu, Y.; Zhao, G.; Chen, J.; Li, H.; Jiang, N.; Hu, D.; Xu, Y.; Zhu, Y.; Nasibulin, A. G. Influence of the filler dimensionality on the electrical, mechanical and electromagnetic shielding properties of isoprene rubber-based flexible conductive composites. *Compos. Commun.* **2020**, *21*, No. 100417.
(35) Ameli, A.; Nofar, M.; Park, C. B.; Pötschke, P.; Rizvi, G. Polypropylene/carbon nanotube nano/microcellular structures with high dielectric permittivity, low dielectric loss, and low percolation threshold. *Carbon* **2014**, *71*, 206−217.
(36) Sun, X.; Liu, X.; Shen, X.; Wu, Y.; Wang, Z.; Kim, J.-K. Reprint of graphene foam/carbon nanotube/poly(dimethyl siloxane) composites for exceptional microwave shielding. *Composites, Part A* **2017**, *92*, 190−197.
(37) Al-Saleh, M. H.; Sundararaj, U. Electromagnetic interference shielding mechanisms of CNT/polymer composites. *Carbon* **2009**, *47*, 1738−1746.
(38) Monnereau, L.; Urbanczyk, L.; Thomassin, J.-M.; Pardoen, T.; Bailly, C.; Huynen, I.; Jérôme, C.; Detrembleur, C. Gradient foaming of polycarbonate/carbon nanotube based nanocomposites with supercritical carbon dioxide and their EMI shielding performances. *Polymer* **2015**, *59*, 117−123.
(39) Zhang, H.; Zhang, G.; Tang, M.; Zhou, L.; Li, J.; Fan, X.; Shi, X.; Qin, J. Synergistic effect of carbon nanotube and graphene nanoplates on the mechanical, electrical and electromagnetic interference shielding properties of polymer composites and polymer composite foams. *Chem. Eng. J.* **2018**, *353*, 381−393.
(40) Li, Y.; Shen, B.; Yi, D.; Zhang, L.; Zhai, W.; Wei, X.; Zheng, W. The influence of gradient and sandwich configurations on the electromagnetic interference shielding performance of multilayered thermoplastic polyurethane/graphene composite foams. *Compos. Sci. Technol.* **2017**, *138*, 209−216.
(41) Kashi, S.; Gupta, R. K.; Baum, T.; Kao, N.; Bhattacharya, S. N. Morphology, electromagnetic properties and electromagnetic inter-

https://doi.org/10.1021/acsomega.2c01293
ACS Omega 2022, 7, 15215−15222

ference shielding performance of poly lactide/graphene nanoplatelet nanocomposites. *Mater. Des.* **2016**, *95*, 119−126.
(42) Jia, X.; Shen, B.; Chen, Z.; Zhang, L.; Zheng, W. High-performance carbonized waste corrugated boards reinforced with epoxy coating as lightweight structured electromagnetic shields. *ACS Sustainable Chem. Eng.* **2019**, *7*, 18718−18725.
(43) Lu, L.; Xing, D.; Teh, K. S.; Liu, H.; Xie, Y.; Liu, X.; Tang, Y. Structural effects in a composite nonwoven fabric on EMI shielding. *Mater. Des.* **2017**, *120*, 354−362.
(44) Sun, X.; He, J.; Li, G.; Tang, J.; Wang, T.; Guo, Y.; Xue, H. Laminated magnetic graphene with enhanced electromagnetic wave absorption properties. *J. Mater. Chem. C* **2013**, *1*, 765−777.
(45) Zhu, S.; Cheng, Q.; Yu, C.; Pan, X.; Zuo, X.; Liu, J.; Chen, M.; Li, W.; Li, Q.; Liu, L. Flexible Fe_3O_4/graphene foam/poly dimethylsiloxane composite for high-performance electromagnetic interference shielding. *Compos. Sci. Technol.* **2020**, *189*, No. 108012.
(46) French, A. D. Idealized powder diffraction patterns for cellulose polymorphs. *Cellulose* **2014**, *21*, 885−896.
(47) Zhang, X.; Ding, W.; Zhao, N.; Chen, J.; Park, C. B. Effects of compressed CO_2 and cotton fibers on the crystallization and foaming behaviors of polylactide. *Ind. Eng. Chem. Res.* **2018**, *57*, 2094−2104.
(48) Zhang, H.; Zhang, G.; Li, J.; Fan, X.; Jing, Z.; Li, J.; Shi, X. Lightweight, multifunctional microcellular PMMA/Fe_3O_4@MWCNTs nanocomposite foams with efficient electromagnetic interference shielding. *Composites, Part A* **2017**, *100*, 128−138.
(49) Lin, J.-H.; Lin, Z.-I.; Pan, Y.-J.; Huang, C.-L.; Chen, C.-K.; Lou, C.-W. Polymer composites made of multi-walled carbon nanotubes and graphene nano-sheets: Effects of sandwich structures on their electromagnetic interference shielding effectiveness. *Composites, Part B* **2016**, *89*, 424−431.

https://doi.org/10.1021/acsomega.2c01293
ACS Omega 2022, 7, 15215−15222